Thallium Mining from Industrial Wastewaters Enabled by a Dynamic Composite Membrane Process

Revised Manuscript

June 22, 2022

Zhangxin Wang[a,b], Shanshan Liu[a], Hailong Zhang[a,b], Zhong Zhang[a,b], Jin Jiang[a,b], Di He [a,b,*], Shihong Lin[c,d,*]

[a]*Key Laboratory for City Cluster Environmental Safety and Green Development of the Ministry of Education, School of Ecology, Environment and Resources, Guangdong University of Technology, Guangzhou, 510006, China*

[b]*Southern Marine Science and Engineering Guangdong Laboratory (Guangzhou), Guangzhou, 511458, China*

[c]*Department of Civil and Environmental Engineering, Vanderbilt University, Nashville, Tennessee 37235-1831, United States*

[d]*Department of Chemical and Biomolecular Engineering, Vanderbilt University, Nashville, Tennessee 37235-1831, United States*

Corresponding author: email: di.he@gdut.edu.cn; shihong.lin@vanderbilt.edu; Tel: +1 (615) 322-7226

Abstract

Thallium (Tl) is a rare but highly toxic element. Mineral exploitation and utilization lead to a risk of thallium (Tl) leakage to the aqueous environment, greatly threatening human health. In this study, we propose a novel Tl wastewater treatment process based on a regenerable adsorptive membrane to achieve Tl removal and recovery from industrial wastewaters. Specifically, a composite membrane was fabricated using Prussian blue (PB) and a commercial polyvinylidene fluoride (PVDF) membrane. The as-fabricated PB/PVDF composite membrane exhibited an outstanding Tl removal efficiency (> 95 %) at various operating conditions (i.e., a permeate flux ≤ 140 L m^{-2} h^{-1}, pH from 3 to 11, and an initial Tl concentration from 50 to 1000 μg/L). Moreover, coexisting heavy metal ions (e.g., Pb^{2+}, Cu^{2+}, Cd^{2+}, Ni^{2+}, and Zn^{2+}) had little interference with the Tl removal efficiency of the PB/PVDF composite membrane. Hydraulic backwash was applied to recover PB-Tl composite particles as a high content source of Tl (92.2 ± 11.4 mg of Tl per gram of composite), while the backwashed PVDF membrane can be reused for the fabrication of the PB/PVDF composite membrane. A simplified economic analysis suggests that chemical cost for synthesizing the consumable Pb in the proposed the dynamic composite membrane process was only ~ 6.1 % of the value of recovered Tl, highlighting the vast potential of the proposed process for Tl removal and recovery from industrial wastewaters.

1. Introduction

Thallium (Tl) is a highly toxic trace element that has attracted increasing attentions in recent years (Liu et al. 2021b, Xu et al. 2019, Zhao et al. 2020). The lethal dose of Tl to human is only 8-10 mg/kg, suggesting a much higher toxicity of Tl than that of other heavy metal elements such as mercury (Hg), cadmium (Cd), and lead (Pb) (Moore et al. 1993, Riyaz et al. 2013). Although typical Tl concentration in natural water is extremely low, Tl could be released to the water environment from exploration and utilization of Tl-bearing mineral resources, and such releases have already resulted in severe Tl contamination incidents (Liu et al. 2019a, Liu et al. 2018, Xu et al. 2019). Furthermore, despite its extreme toxicity, Tl is a valuable element that has been utilized in electronic, optical, and superconducting materials industries (Ning et al. 2021, Peter and Viraraghavan 2005). Considering the rareness of Tl in natural minerals, mining Tl from Tl-containing industrial wastewaters (e.g., metallurgical wastewater, sulfuric acid production wastewater, and mine water) becomes a very appealing option (Hermassi et al. 2022, Lin et al. 2021, Liu et al. 2019a).

In water, Tl exists in the form of Tl^{+} and/or Tl^{3+}. As Tl^{3+} can be readily hydrolyzed and removed through adsorption and coprecipitation processes (Liu et al. 2021b, Liu et al. 2019b), the removal of Tl^{+} is the major challenge and thus the focus of this study (i.e., Tl removal hereafter will specifically refer to the removal of Tl^{+}). A variety of wastewater treatment technologies, including chemical precipitation/coagulation, oxidation-reduction precipitation, ion exchange, adsorption, solvent extraction, and microbial fuel cells have been investigated for removing Tl from wastewaters (Huangfu et al. 2015, Li et al. 2019, Liu et al. 2019a, Xu et al. 2019, Zhang et al. 2018a). Among these technologies, adsorption is the most promising as it has the advantages of high Tl removal efficiency, low operating cost, and thus high economic viability (Xu et al.

2019). Based on previous studies, Prussian blue (PB) has been recognized as a highly effective absorbent because it can absorb Tl from wastewaters efficiently and selectively in the presence of other co-existing cations (Lopez et al. 2021, Zhang et al. 2022). However, the separation of the PB-Tl composite from the wastewaters after Tl adsorption is a technical challenge especially for large-scale applications (Vipin et al. 2016, Zhang et al. 2022).

Microfiltration (MF) is a commercially mature membrane filtration technology that can separate micron-sized solids from the liquids (Baker 2012, Mulder 1996). A variety of advanced water/wastewater treatment technologies have been developed by coupling MF with other processes (Juang et al. 2013, Mori et al. 1998, Zuo et al. 2018). For instance, by growing specific microorganisms on MF membranes as the substrates, membrane bioreactors (MBR) have been developed and now widely employed (Judd 2008, Smith et al. 2012). Compared to other biological wastewater treatment technologies, MBR has the advantages of high-quality effluent and higher volumetric loading rates (Jegatheesan et al. 2016, Xiao et al. 2019). In addition, MF has been combined with granular activated carbon (GAC) to form hybrid MF-GAC systems for water/wastewater purifications (Kim et al. 2009, Shanmuganathan et al. 2015). Inspired by the approach adopted in MBR and hybrid MF-GAC systems, a composite membrane with a PB surface layer and an MF membrane substrate could potentially overcome the challenge of separating the PB-Tl composite from wastewaters and recover PB-Tl composite with a high Tl content as a high-value source of Tl.

In this study, we develop a novel process using a PB/polyvinylidene fluoride (PVDF) composite membrane to recover Tl from wastewaters as a high-value mineral. The PB/PVDF composite membrane is fabricated by filtering a PB dispersion through a commercial PVDF MF membrane, and its morphology is characterized. Then, we

assess the Tl removal performance of the PB/PVDF composite membrane at varied operating conditions (i.e., permeate flux, pH, Tl concentration, presence of co-existing heavy metal ions, and cumulative filtrate volume). Further, we decompose the PB/PVDF composite membrane via hydraulic backwash and quantify the Tl content in the recovered PB-Tl composite. Based on these results, we propose a dynamic composite membrane process for Tl recovery from industrial wastewaters and perform a simple economic analysis to estimate the application potential of the proposed process.

2. Materials and methods

2.1. Materials

The MF membranes used in this study were commercial hydrophilic PVDF membranes with a nominal pore size of 0.22 μm (Haining Chuangwei Filtration Equipment, China). Potassium hexacyanoferrate (II) trihydrate ($K_4[Fe(CN)_6]\cdot 3H_2O$), ferric chloride ($FeCl_3$), nickel chloride hexahydrate ($NiCl_2\cdot 6H_2O$), and cadmium chloride ($CdCl_2$) were purchased from Aladdin (Shanghai, China). Sodium hydroxide (NaOH) was obtained from Macklin Co. Ltd. (China). Nitric acid (HNO_3) was purchased from Guangzhou Brand Chemical Reagent (Guangzhou, China). The standard Tl solution containing 1000 mg/L Tl^+ was obtained from the Groups of the General Research Institute for Nonferrous Metals (China). All the reagents were analytical reagent grade and used as received without any further treatment, and deionized (DI) water was used to prepare the solutions.

2.2. Fabrication of the PB/PVDF composite membrane

The fabrication procedure of the PB/PVDF composite membrane is illustrated in Fig. 1A. Specifically, a PB suspension was prepared by mixing 0.0075 g

$K_4[Fe(CN)_6]\cdot 3H_2O$ and 0.0039 g $FeCl_3$ in 50 mL DI water (detailed chemical reaction in the Supplementary Materials). Then, the prepared PB suspension was transferred to a dead-end filtration cell with a PVDF membrane coupon with an area of 12.56 cm^2. Nitrogen gas was applied to pressurize the PB suspension (20 kPa) and drive the water through the PVDF membrane. After filtration, a layer of PB solids was retained on the PVDF membrane surface, resulting in the PB/PVDF composite membrane. The PB content in the as-fabricated PB/PVDF composite membrane was estimated to be 4.06 g/m^2 (detailed calculation in the Supplementary Materials).

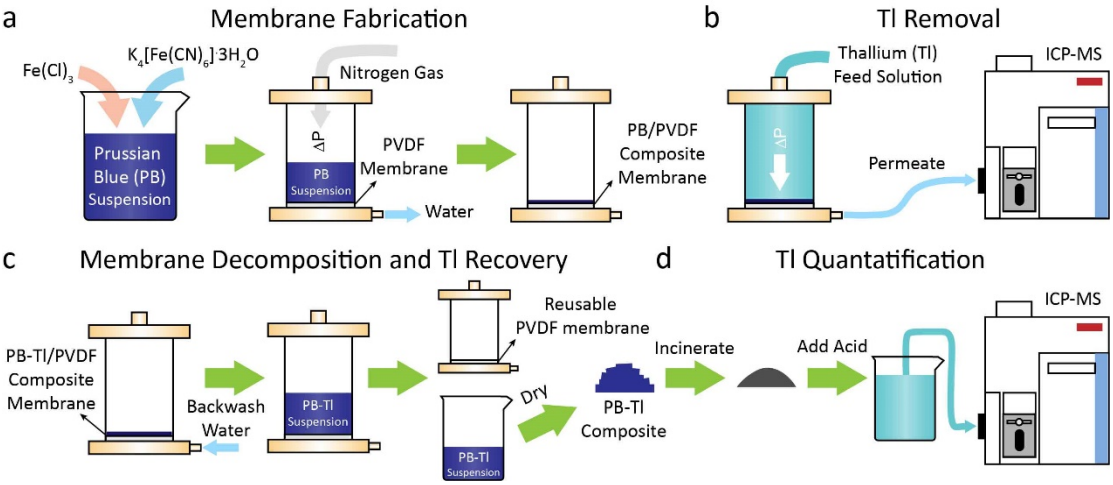

Fig. 1 Schematic illustration of the experimental procedures. (A) Fabrication of the PB/PVDF composite membrane. (B) Tl removal from the wastewater via membrane filtration. (C) Decomposition of the PB/PVDF composite membrane and recovery of the PB-Tl composite. (D) Quantification of the Tl content in the recovered PB-Tl composite.

2.3. Membrane characterizations

The morphology of the PB/PVDF composite membrane was observed using scanning electron microscopy (SEM, LTRA 3 XMU, Tescan). The structure of the synthesized PB was characterized by X-ray diffraction (XRD, Rigaku Ultima IV X-ray diffractometer) using CuKα radiation at 3kW, and the data was collected at angles (2θ)

143 from 10° to 80° with a scanning rate of 2° min^{-1}. The water permeabilities of the pristine
144 PVDF membrane and PB/PVDF composite membrane were determined using dead-
145 end filtration experiments with DI water (detailed procedures reported in
146 Supplementary Materials).

147 *2.3. Tl removal via membrane filtration*

148 Dead-end filtration experiments were conducted to determine the Tl removal
149 capability of the PB/PVDF composite membrane at varied experimental conditions (Fig.
150 1B). Four sets of short-term experiments were performed to investigate the impact of
151 operating conditions on the Tl removal efficiency of the PB/PVDF composite
152 membrane. The first set of short-term experiments were performed using a feed solution
153 containing 1 mg L^{-1} Tl with varied permeate fluxes (i.e., from 50 to 430 L m^{-2} h^{-1}) at
154 pH 3.0. The varied permeate fluxes were obtained by applying different hydraulic
155 pressures, and the dependence of permeate flux on hydraulic pressure can be found in
156 the Supplementary Materials (Fig. S1b). The second set of short-term experiments were
157 performed using Tl feed solutions of different initial concentrations (i.e., from 10 to
158 1000 μg L^{-1}) with a permeate flux of ~100 L m^{-2} h^{-1} at pH 3.0. The third set of short-
159 term experiments were performed using 1 mg L^{-1} Tl feed solution with a permeate flux
160 of ~100 L m^{-2} h^{-1} at varied pH (i.e., from 3 to 12). The fourth set of short-term
161 experiments were performed using 1 mg L^{-1} Tl feed solutions containing different co-
162 existing heavy metal ions (i.e., Pb^{2+}, Cu^{2+}, Cd^{2+}, Ni^{2+}, and Zn^{2+}) of different
163 concentrations (from 10 to 1000 mg L^{-1}) with a permeate flux of ~100 L m^{-2} h^{-1} at pH
164 3.0. It should be noted that pH 3.0 was chosen as the experimental pH to avoid the

formation of metal hydroxides.

In each short-term experiment, 100 mL of feed solution was used, and after 60 mL of the permeate was produced, the Tl concentration in the permeate stream (c_P) was measured by inductively coupled plasma mass spectroscopy (ICP-MS, Thermo Scientific iCAP Q). The calibration of ICP-MS was performed using the standard Tl solution, and Bi (10 μg L^{-1}) was used as the internal standard for analysis. The Tl removal rate of the PB/PVDF composite membrane (R_{Tl}) was calculated as follow,

$$R_{Tl} = (1 - \frac{c_P}{c_0}) \times 100\% \quad (1)$$

where c_0 is the initial Tl concentration in the feed solution.

In addition to short-term experiments, a long-term experiment was also performed to investigate the Tl removal capacity of the PB/PVDF composite membrane. The long-term experiment was performed with a permeate flux of ~100 L m^{-2} h^{-1} using 2 L feed solution containing 1 mg L^{-1} Tl^{+} at pH 3.0. During the long-term experiment, the Tl concentration in the permeate stream was measured by ICP-MS after every 60 mL of permeate was produced, and the corresponding Tl removal efficiency was calculated using Eq. 1. Once the Tl removal efficiency was below 30 %, the long-term experiment was terminated, and based on the experimental result, the time duration of the long-term experiment was ~12 hours.

2.4. Tl recovery and regeneration of PVDF membrane

After the membrane filtration test, PB with adsorbed Tl was recovered from the composite membrane using hydraulic backwash (Fig. 1C). Specifically, 10 mL DI water was used to backwash with a hydraulic pressure of 100 kPa to obtain a suspension of

PB-Tl and a regenerated PVDF membrane. Solid PB-Tl composite was obtained by drying the suspension at 80 °C for 6 hours, and the regenerated PVDF membrane can be used for next cycle of PB/PVDF membrane formation and Tl recovery.

2.5. Quantification of the Tl content in the recovered PB-Tl composite

The Tl content in the PB-Tl composite was quantified to determine the quality of the recovered Tl resource (Fig. 1D). First, the mass of the PB-Tl composite (m_c) was measured using an analytical balance. Then, the PB-Tl composite was incinerated in a muffle oven at 400 °C for 4 h. The residue from incineration was completely dissolved in HNO_3 (0.1 M) under heating, and the total volume of the resulted solution (V_s) was recorded. By determining the Tl concentration in the resulted solution (c_s) using ICP-MS (detailed procedures described in Section 2.3), the Tl content in the PB-Tl composite (f_{Tl}) was obtained,

$$f_{Tl} = \frac{c_s V_s}{m_c} \times 100\% \quad (2)$$

3. Results and discussion

3.1. Characterizations of the PB/PVDF composite membrane

The PB deposit on the PVDF membrane surface appears dark blue (Fig. 2a). The morphology of the composite membrane is further unveiled by the SEM images. The top surface of the composite membrane is a dense and uniform layer formed by packing of small nanocages (Fig. 2b). The substrate PVDF membrane exhibits a microporous structure unaffected by the PB deposition (Fig. 2c). A distinct boundary between the PB surface coating and the substrate PVDF membrane is observed from the cross-section SEM image of the composite membrane (Fig. 2d), which suggests no or minimal intrusion of PB particles into the substrate membrane.

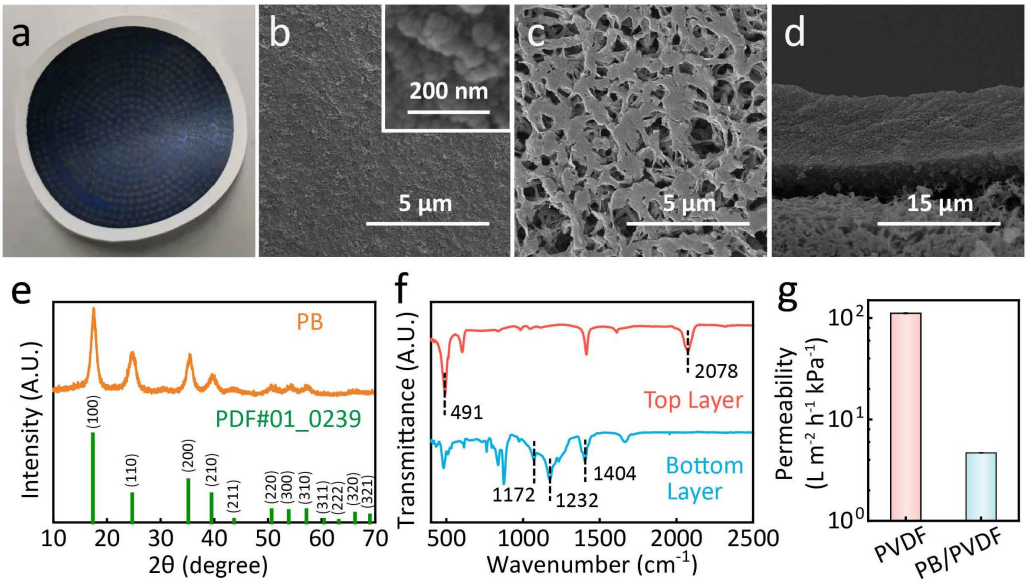

Fig. 2 Characterizations of the PB/PVDF composite membrane. (a) Photographic image of the PB/PVDF composite membrane. SEM images featuring the (b) top surface (i.e., PB surface layer), (c) bottom surface (i.e., PVDF membrane substrate), and (d) cross-section morphology of the PB/PVDF composite membrane. The inset in panel (b) denotes the local surface morphology at a larger magnification. (e) XRD pattern of the PB surface layer. (f) FTIR spectra of the top layer (red curve) and bottom layer (blue curve) of the PB/PVDF composite membrane. (g) Water permeabilities of the PVDF membrane (red column) and PB/PVDF composite membrane (blue column).

XRD analysis confirms the surface layer to be exactly PB (PDF#01_0239, Fig. 2e), (Wu et al. 2018, Zhang et al. 2012). The PB surface layer was further verified by FTIR characterization (Fig. 2f). For the bottom layer, the peaks at 491 and 2078 cm^{-1} can be attributed to the vibrations of Fe(II)-C≡N-Fe(III) and -C≡N- groups, respectively, suggesting that the top layer was comprised of PB (Zhang et al. 2022). For the bottom layer, the peaks at 1172, 1232, and 1405 cm^{-1} can be ascribed to the vibrations of -CF2-, indicating that the bottom layer is the commercial PVDF membrane (Boccaccio et al. 2002). The membrane morphology and chemical composition analysis confirm the successful fabrication of PB/PVDF composite membrane.

To evaluate the impact of the PB surface layer on the filtration performance of the composite membrane, both the water permeabilities of the pristine PVDF membrane and PB/PVDF composite membrane were measured (details in the Supplementary

Materials). As Fig. 2g shows, the water permeability of the PB/PVDF composite membrane (4.7 ± 0.1 L m^{-2} h^{-1} kPa^{-1}) is significantly lower than that of the pristine PVDF membrane (111.5 ± 2.0 L m^{-2} h^{-1} kPa^{-1}), because the PB surface layer adds a significant resistance to water permeation.

3.2. Tl removal with the PB/PVDF composite membrane

3.2.1 Impact of permeate flux on Tl removal

The impact of permeate flux on the Tl removal efficiency of the PB/PVDF composite membrane was investigated (Fig. 3a). With a permeate flux lower than 140 L m^{-2} h^{-1}, a high Tl removal efficiency (> 97 %) was achieved. Since the Tl removal efficiency of the pristine PVDF membrane is negligible (details in the Supplementary Materials), the excellent Tl removal capability of the PB/PVDF composite membrane is attributed to the adsorption by the PB layer, a process that has been extensively studied in literatures (Lehmann and Favari 1984, Mohammad et al. 2014, Yang et al. 2008). As the permeate flux further increased (i.e., >140 L m^{-2} h^{-1}), the Tl removal efficiency drastically decreased likely due to the shortened hydraulic retention time and reduced contact between the Tl ions and the PB layer. Based on the above analysis, a moderate permeability flux (~100 L m^{-2} h^{-1}) was chosen for all membrane filtration experiments discussed in the following sections.

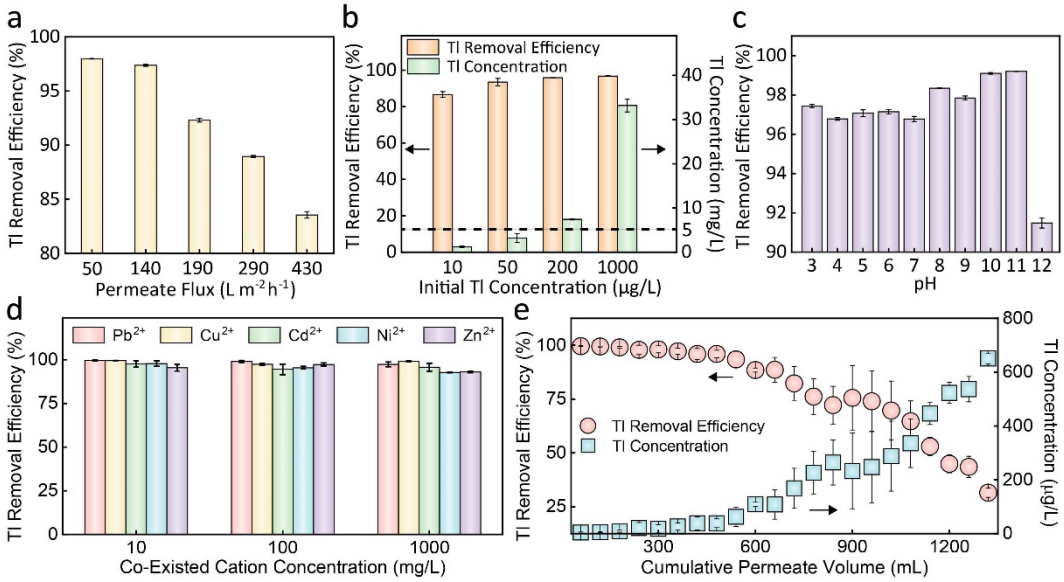

Fig. 3 Tl removal capability of the PB/PVDF composite membrane. (a) Impact of permeate flux on the Tl removal efficiency. In each experiment, the initial Tl concentration and pH of the feed solution were 1 mg/L and 3, respectively. (b) Impact of initial Tl concentration on the Tl removal efficiency (orange columns, left vertical axis) and the corresponding Tl concentration in the permeate stream (green columns, right vertical axis). In each experiment, the permeate flux and the pH of the feed were controlled at ~100 L m^{-2} h^{-1} and 3, respectively. (c) Impact of pH on the Tl removal efficiency. In each experiment, the permeate flux and initial Tl concentration of the feed solution were set at ~100 L m^{-2} h^{-1} and 1 mg/L, respectively. (d) Impact of co-existing ions on the Tl removal efficiency. Five representative ions, Pb^{2+} (red columns), Cu^{2+} (yellow columns), Cd^{2+} (blue columns), Zn^{2+} (green columns), and Fe^{2+} (purple columns) were used as the co-existing ions in the measurements, and for each ion, the concentration varied from 10 to 1,000 mg/L. In each measurement, the initial Tl concentration and pH of the feed solution were 1 mg/L and 3, respectively, and the permeate flux was controlled at ~100 L m^{-2} h^{-1}. In panels (a), (b), (c), and (d), each Tl removal efficiency was determined via measuring the Tl concentration in the permeate stream after 60 mL permeate was produced. (e) Tl removal efficiency (red circles, left vertical axis) and Tl concentration in the permeate stream (blue squares, right vertical axis) as a function of the cumulative permeate volume. In the experiment, the initial Tl concentration and pH of the feed solution were 1 mg/L and 3, respectively, and the permeate flux was controlled at ~100 L m^{-2} h^{-1}. The Tl removal efficiency was determined via measuring the Tl concentration in the permeate stream after every 60 mL of permeate was produced.

3.2.2 Impact of Tl concentration on Tl removal

To evaluate the performance of the PB/PVDF composite membrane on treating different Tl wastewaters, the Tl removal efficiencies of the PB/PVDF composite membrane were determined using feed solutions with varied initial Tl concentrations. With increasing initial Tl concentration, the Tl removal efficiency increases (orange columns in Fig. 3b), yet the effluent Tl concentration also increases (green columns in Fig. 3b).

The maximum allowable Tl concentrations for industrial wastewater discharge are 140 and 5 μg L^{-1} in US and China, respectively (Liu et al. 2019a). Results from Fig. 3b suggest that, as long as the feed Tl concentration does not exceed 200 μg L^{-1}, using the PB/PVDF membrane with the selected operating condition can meet the discharge standards in both the US and China. For higher feed concentration (e.g., >200 μg L^{-1}) and stringent discharge standard (e.g., <5 μg L^{-1}), compliance of effluent quality can be achieved by increasing the Tl-Pb contact time via using a slower filtration rate or employing multi-stage filtration (Fig. S4 in the Supplementary Materials).

3.2.3 Impact of pH on Tl removal

Since Tl wastewaters could come from a variety of different sources, the pH of the wastewaters can vary substantially (Pavoni et al. 2018) and its impact on Tl removal was thus investigated. The Tl removal efficiencies of the PB/PVDF composite membrane were evaluated at pH from 3 to 12 (Fig. 3c). As pH increased from 3 to 11, the Tl removal efficiency remained relatively steady (> 96 %). The Tl removal efficiency was compromised only when pH increased beyond 12 as the PB structure was destructed under such an alkaline condition (Fig. S5 in the Supplementary Materials). Based on previous studies, the destruction of PB can be explained by its reaction with hydroxide ions that produces ferric hydroxide and ferrocyanide (Koncki et al. 2001, Koncki and Wolfbeis 1998). These results suggest that the PB/PVDF composite membrane is functional over a wide range of pH except for highly alkaline conditions.

3.2.4 Impact of co-existing cations on Tl removal

Tl wastewaters usually contain other heavy metal ions that co-exist with Tl in the source minerals (Liu et al. 2021a, Luo et al. 2020, Tatsi and Turner 2014). Thus, the impact of co-existing cations on Tl removal by the PB/PVDF composite membrane was

305 investigated. Five representative heavy metal ions (i.e., Pb^{2+}, Cu^{2+}, Cd^{2+}, Ni^{2+}, and Zn^{2+})
306 were employed to evaluate the Tl removal efficiencies of the PB/PVDF composite
307 membrane in the presence of co-existing heavy metal ions (Fig. 4d). In the feed
308 solutions, the concentration of the co-existing heavy metal ions varies from 10 to 1000
309 mg L^{-1}, which is 10 to 1000 times higher than the Tl concentration (i.e., 1 mg L^{-1}).
310 However, the Tl removal efficiency still exceeded 90 % in all cases regardless of the
311 co-existing ion species or concentrations (Fig. 4d), suggesting that the adsorption of Tl
312 by the PB/PVDF composite membrane is highly selective. The exact mechanism of the
313 high Tl selectivity of PB has not be fully elucidated. Previous studies have attributed
314 the selectivity of PB toward Tl^{+} adsorption to the favorable ion exchange between Tl^{+}
315 and K^{+} on PB lattices (Lopez et al. 2021, Zhao et al. 2020). More recent work revealed
316 that that ion dehydration might also play an important role in the selective Tl removal
317 of PB against other ions as the dehydrated Tl^{+} can more easily enter the crystal lattices
318 of PB (Zhang et al. 2022).

319 *3.2.5 Tl adsorption capacity*

320 The capacity of the PB/PVDF composite membrane for Tl removal is limited as
321 the removal mechanism is adsorption instead of rejection (Khulbe and Matsuura 2018,
322 Yang et al. 2021, Zhang et al. 2018b). The Tl removal capacity of the PB/PVDF
323 composite membrane was determined by a long-term filtration experiment using a 1
324 mg L^{-1} Tl feed solution. When the cumulative permeate volume was less than 540 mL,
325 the Tl removal efficiency could remain stable and high (~ 95 %), and the Tl
326 concentration in the permeate stream was less than 50 μg L^{-1}. When the cumulative
327 permeate volume exceeded 540 mL, a gradual increase in permeate Tl concentration
328 was observed, which suggests that the top portion of the PB layer started to become
329 saturated. Continued filtration of Tl wastewater further extended the saturation zone

and reduced the Tl removal efficiency. If we set 540 mL as the cumulative permeate volume below which the permeate quality (i.e., Tl concentration) is considered as compliant, the Tl content in the PB layer (i.e., PB-Tl composite) is calculated to be 95.8 ± 9.6 mg g^{-1} (details in the Supplementary Materials). After Tl adsorption, the PB/PVDF composite membrane could maintain its structure (Fig. 2d and Fig. S6).

3.2.5 Regeneration of the PB/PVDF composite membrane and Tl recovery

Due to the strong attraction between PB and Tl, in-situ desorption of Tl from PB is highly challenging (Zhao et al. 2020). Since the binding of the PB layer and PVDF membrane substrate is weak (Fig. 2D), the PB/PVDF composite membrane can be regenerated by removing the PB-Tl composite layer and reconstructing the PB layer on the PVDF membrane surface. Specifically, hydraulic backwash with DI water was applied to detach the PB-Tl composite layer from the PVDF membrane after TI adsorption, and the performance of the reconstructed PB/PVDF composite membrane was evaluated (Fig. 4a). The regenerated PB/PVDF membrane was tested for a cumulative permeate volume of 540 mL with a feed Tl concentration of 1 mg L^{-1}.

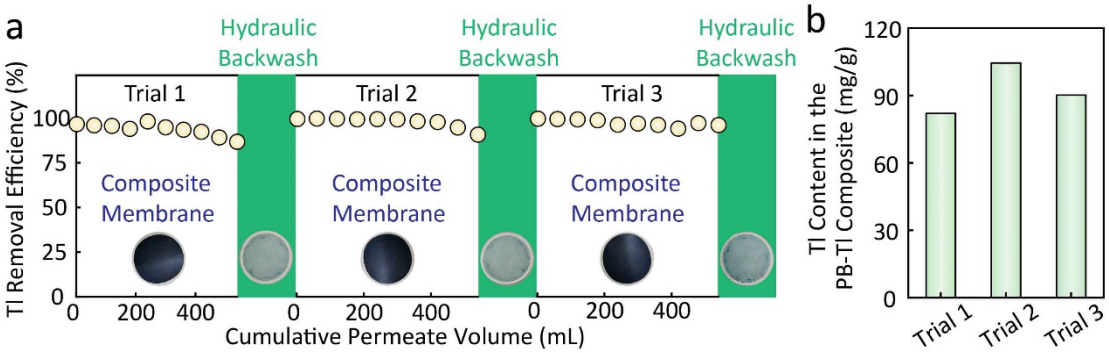

Fig. 4 Regeneration of the PB/PVDF composite membrane and Tl recovery. (a) Tl removal efficiency as a function of cumulative permeate volume in the membrane filtration experiment by repeatedly constructing and decomposing the PB/PVDF composite membrane for 3 times (i.e., 3 trials). In each trial, the PB/PVDF composite membrane was first constructed, and then tested with a permeate flux of ~100 L m^{-2} h^{-1} using 1 mg/L Tl feed solution at pH 3.0. After 540 mL of the permeate was produced, the PB/PVDF composite membrane was decomposed by hydraulic backwash using 20 mL DI water. The photographic images depict the membrane at different stages. (b) Measured Tl content in the PB-Tl composite obtained from each trial. In each trial, the PB-Tl composite was obtained after drying the suspension from hydraulic

backwash.

The performance of the Tl removal was reproduceable using the regenerated PB/PVDF membrane (Fig. 4a). Photographic images in Fig. 4a show that the PB/PVDF composite membrane can be mostly removed by hydraulic backwash using DI water (as indicated by the almost complete disappearance of the dark blue top layer after backwash). As mentioned earlier, the easy detachment of the PB layer from the PVDF substrate can be attributed to their weaking binding. Once the PB/PVDF composite membrane was reconstructed, the Tl removal efficiency was restored. In all three trials of Tl removal using regenerated PB/PVDF composite membrane, outstanding Tl removal capability was observed, demonstrating the viability of PB/PVDF composite membrane regeneration.

After hydraulic backwash, the PB layer with adsorbed Tl was removed from the PVDF membrane substrate as a suspension of PB-Tl composite. Since PB has a relatively large Tl adsorption capacity (Fig. 3e), the PB-Tl composite has the potential to be recovered Tl resource. The Tl content in the PB-Tl composite was measured to be 92.2 ± 11.4 mg/g (Fig. 4b), which is consistent with the Tl adsorption capacity of PB (95.8 ± 9.6 mg/g). In comparison, the Tl contents in natural minerals are usually lower than 20 mg/g, significantly lower than that in the PB-Tl composite (Baceva et al. 2014, Dordevic et al. 2021). Thus, in terms of Tl content, the PB-Tl composite can be considered as a high-grade Tl mineral.

3.4. Dynamic PB/PVDF Composite Membrane for Tl Recovery from Wastewaters

Based on the experimental results presented in this study, a dynamic composite membrane process is proposed for Tl removal and recovery from wastewaters using full-scale membrane modules (Fig. 5a). The proposed process consists of three stages: PB layer formation, adsorptive filtration of Tl, and hydraulic backwash. For PB layer

formation, a suspension of PB synthesized using $FeCl_3$ and $K_4[Fe(CN)_6]\cdot 3H_2O$ is filtered by a commercial PVDF membrane module to form a top PB layer for Tl adsorption. Through adsorptive filtration, Tl in the wastewater is efficiently removed by the PB layer on the PB/PVDF composite membrane. Once the PB layer is partially saturated with adsorbed Tl to the extent that the permeate quality is non-compliant, hydraulic backwash with freshwater is applied to remove the PB-Tl composite on the PVDF membrane and recover it in the form of a suspension. Drying the suspension recovers the PB-Tl composite as a high-content source of Tl. The backwashed PVDF membrane module can be reused for the formation of new PB/PVDF composite membrane module, which starts the next cycle of Tl recovery. We note that the formation of new PB/PVDF membrane involves only the filtration of a PB suspension and can be achieved practically even with commercial membrane modules.

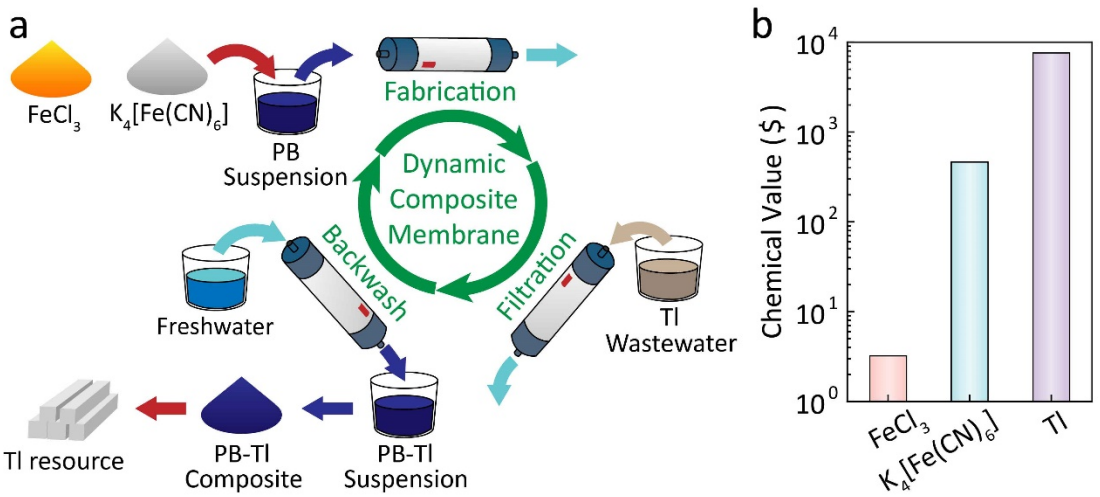

Fig. 5 Tl wastewater treatment enabled by a dynamic composite membrane. (a) Schematic illustration of the dynamic PB/PVDF composite membrane process. (b) A simple economic analysis of the chemicals involved in the dynamic composite membrane process. The analysis was conducted based on the assumption that 1 kg Tl was recovered.

To further evaluate the economic viability of this dynamic composite membrane process, a simplified economic analysis was performed based on the values of chemicals used and recovered (Fig. 5b). The analysis is based on recovering 1 kg of Tl

which has a value of ~$ 7,600 according to literature (Reilly 2020). Based on the Tl content in the PB-Tl composite (Fig. 4b), recovering 1 kg of Tl requires 9.49 kg of PB the synthesis of which consumes 7.17 kg of $FeCl_3$ and 14.01 kg of $K_4[Fe(CN)_6]\cdot 3H_2O$. Since the price of $FeCl_3$ and $K_4[Fe(CN)_6]\cdot 3H_2O$ are $ 0.45 and $ 33.00 per kilogram, respectively (from www.alibaba.com), the total cost of $FeCl_3$ and $K_4[Fe(CN)_6]\cdot 3H_2O$ required to recover 1 kg of Tl is estimated to be $ 465.56, accounting for only 6.1% of the value of the recovered Tl. While such an analysis only considers the costs of the core materials, the high value of Tl and the very low cost of the core materials for synthesizing the adsorbent suggests a strong potential for the proposed dynamic composite membrane process to be economically viable. To fully evaluate the economic competitiveness of the process, a more comprehensive technoeconomic analysis based on data from pilot-scale investigation is required, which is beyond the scope of the current study.

4. Conclusions

A dynamic composite membrane process has been demonstrated for Tl removal and recovery from industrial wastewaters. Specifically, a PB/PVDF composite membrane comprising a PB surface layer and a PVDF membrane substrate has been shown to be able to effectively remove Tl from wastewaters of different Tl concentrations (i.e., 50-1000 μg L^{-1}) over a wide range of pH (i.e., 3-11). The adsorption of Tl was highly selective with minimal interference from co-existing heavy metal ions at much higher concentrations. The Tl removal rate of the PB/PVDF composite membrane was over 90 % until the PB layer was partially saturated (corresponding to a Tl content of 95.8 ± 9.6 mg g^{-1} in this study). The PB layer with adsorbed Tl can be readily removed and recovered as a high-content source of Tl with simple hydraulic

backwash, while the backwashed PVDF membrane can be reused for forming a new PB/PVDF composite membrane for next-cycle Tl recovery. A simple economic analysis based on the costs of Tl and adsorbents suggests that the proposed dynamic composite membrane process has a strong potential to become an economically competitive process for Tl removal and recovery from industrial wastewaters.

Acknowledgement

Z.W. and J. J. acknowledge the support from the Program for Guangdong Introduction of Innovative and Entrepreneurial Teams (2019ZT08L213). Z.W. acknowledges the support from the National Science Foundation of China (52100079). Z.W. and D. H. acknowledge the support from the Science and Technology Planning Project of Guangdong Province (2021A0505110013). S. Lin acknowledges the support from the Water Research Foundation via the Paul L. Busch Award and from the National Science Foundation via Grant #1903685.

References

Baceva, K., Stafilov, T., Sajn, R., Tanaselia, C. and Makreski, P. (2014) Distribution of chemical elements in soils and stream sediments in the area of abandoned Sb-As-Tl Allchar mine, Republic of Macedonia. Environmental Research 133, 77-89.

Baker, R.W. (2012) Membrane Technology and Applications, John Wiley & Sons, Hoboken, NJ.

Boccaccio, T., Bottino, A., Capannelli, G. and Piaggio, P. (2002) Characterization of PVDF membranes by vibrational spectroscopy. Journal of Membrane Science

210(2), 315-329.

Dordevic, T., Drahota, P., Kolitsch, U., Majzlan, J., Peresta, M., Kiefer, S., Stoger-Pollach, M., Tepe, N., Hofmann, T., Mikus, T., Tasev, G., Serafimovski, T., Boev, I. and Boev, B. (2021) Synergetic Tl and As retention in secondary minerals: An example of extreme arsenic and thallium pollution. Applied Geochemistry 135.

Hermassi, M., Granados, M., Valderrama, C., Ayora, C. and Cortina, J.L. (2022) Recovery of rare earth elements from acidic mine waters: An unknown secondary resource. Science of the Total Environment 810.

Huangfu, X.L., Jiang, J., Lu, X.X., Wang, Y., Liu, Y.Z., Pang, S.Y., Cheng, H.J., Zhang, X. and Ma, J. (2015) Adsorption and Oxidation of Thallium(I) by a Nanosized Manganese Dioxide. Water Air and Soil Pollution 226(1).

Jegatheesan, V., Pramanik, B.K., Chen, J.Y., Navaratna, D., Chang, C.Y. and Shu, L. (2016) Treatment of textile wastewater with membrane bioreactor: A critical review. Bioresource Technology 204, 202-212.

Juang, Y.J., Nurhayati, E., Huang, C.P., Pan, J.R. and Huang, S.M. (2013) A hybrid electrochemical advanced oxidation/microfiltration system using BDD/Ti anode for acid yellow 36 dye wastewater treatment. Separation and Purification Technology 120, 289-295.

Judd, S. (2008) The status of membrane bioreactor technology. Trends in Biotechnology 26(2), 109-116.

470 Khulbe, K.C. and Matsuura, T. (2018) Removal of heavy metals and pollutants by
471 membrane adsorption techniques. Applied Water Science 8(1).

472 Kim, K.Y., Kim, H.S., Kim, J., Nam, J.W., Kim, J.M. and Son, S. (2009) A hybrid
473 microfiltration-granular activated carbon system for water purification and
474 wastewater reclamation/reuse. Desalination 243(1-3), 132-144.

475 Koncki, R., Lenarczuk, T., Radomska, A. and Glab, S. (2001) Optical biosensors
476 based on Prussian Blue films. Analyst 126(7), 1080-1085.

477 Koncki, R. and Wolfbeis, O.S. (1998) Composite films of Prussian Blue and N-
478 substituted polypyrroles: Fabrication and application to optical determination of
479 pH. Analytical Chemistry 70(13), 2544-2550.

480 Lehmann, P.A. and Favari, L. (1984) Parameters for the adsorption of thallium ions
481 by activated charcoal and Prussian blue. J Toxicol Clin Toxicol 22(4), 331-339.

482 Li, H.S., Zhang, H.G., Long, J.Y., Zhang, P. and Chen, Y.H. (2019) Combined Fenton
483 process and sulfide precipitation for removal of heavy metals from industrial
484 wastewater: Bench and pilot scale studies focusing on in-depth thallium removal.
485 Frontiers of Environmental Science & Engineering 13(4).

486 Lin, S.H., Hatzell, M., Liu, R.P., Wells, G. and Xie, X. (2021) Mining resources from
487 water. Resources Conservation and Recycling 175.

488 Liu, J., Luo, X.W., Sun, Y.Q., Tsang, D.C.W., Qi, J.Y., Zhang, W.L., Li, N., Yin, M.L.,

Wang, J., Lippold, H., Chen, Y.H. and Sheng, G.D. (2019a) Thallium pollution in China and removal technologies for waters: A review. Environment International 126, 771-790.

Liu, J., Wang, J., Tsang, D.C.W., Xiao, T.F., Chen, Y.H. and Hou, L.P. (2018) Emerging Thallium Pollution in China and Source Tracing by Thallium Isotopes. Environmental Science & Technology 52(21), 11977-11979.

Liu, Y., Wei, L.Z., Luo, D.G., Xiao, T.F., Lekhov, A., Xie, X.M., Huang, X.X. and Su, X.T. (2021a) Geochemical distribution and speciation of thallium in groundwater impacted by acid mine drainage (Southern China). Chemosphere 280.

Liu, Y.L., Li, Y.T., Wang, L., Wang, W. and Ma, J. (2021b) Enhanced Trace Tl Removal with Ferrate through the Addition of Mn(II): Effect and Mechanism. ACS ES&T Engineering 1(3), 571-580.

Liu, Y.L., Zhang, J., Huang, H.M., Huang, Z.S., Xu, C.B., Guo, G.J., He, H.Y. and Ma, J. (2019b) Treatment of trace thallium in contaminated source waters by ferrate pre-oxidation and poly aluminium chloride coagulation. Separation and Purification Technology 227.

Lopez, Y.C., Ortega, G.A., Martinez, M.A. and Reguera, E. (2021) Magnetic Prussian Blue derivative like absorbent cages for an efficient thallium removal. Journal of Cleaner Production 283.

Luo, C., Routh, J., Dario, M., Sarkar, S., Wei, L.Z., Luo, D.G. and Liu, Y. (2020)

Distribution and mobilization of heavy metals at an acid mine drainage affected region in South China, a post-remediation study. Science of the Total Environment 724.

Mohammad, A., Faustino, P.J., Khan, M.A. and Yang, Y. (2014) Long-term stability study of Prussian blue - a quality assessment of water content and thallium binding. Int J Pharm 477(1-2), 122-127.

Moore, D., House, I. and Dixon, A. (1993) Thallium poisoning. Diagnosis may be elusive but alopecia is the clue. British Medical Journal 306(6891), 1527.

Mori, Y., Oota, T., Hashino, M., Takamura, M. and Fujii, Y. (1998) Ozone-microfiltration system. Desalination 117(1-3), 211-218.

Mulder, M. (1996) Basic principles of membrane technology, Springer, Dordrecht, Netherlands.

Ning, Z.P., Liu, E.G., Yao, D.J., Xiao, T.F., Ma, L., Liu, Y.Z., Li, H. and Liu, C.S. (2021) Contamination, oral bioaccessibility and human health risk assessment of thallium and other metal(loid)s in farmland soils around a historic Tl-Hg mining area. Science of the Total Environment 758.

Pavoni, E., Covelli, S., Adami, G., Baracchini, E., Cattelan, R., Crosera, M., Higueras, P., Lenaz, D. and Petranich, E. (2018) Mobility and fate of Thallium and other potentially harmful elements in drainage waters from a decommissioned Zn-Pb mine (North-Eastern Italian Alps). Journal of Geochemical Exploration 188, 1-10.

529 Peter, A.L.J. and Viraraghavan, T. (2005) Thallium: a review of public health and
530 environmental concerns. Environment International 31(4), 493-501.

531 Reilly, J.F. (2020) Mineral Commodity Summaries 2020, U.S. Geological Survey,
532 Reston, Virginia.

533 Riyaz, R., Pandalai, S.L., Schwartz, M. and Kazzi, Z.N. (2013) A Fatal Case of
534 Thallium Toxicity: Challenges in Management. Journal of Medical Toxicology 9(1),
535 75-78.

536 Shanmuganathan, S., Johir, M.A.H., Nguyen, T.V., Kandasamy, J. and Vigneswaran,
537 S. (2015) Experimental evaluation of microfiltration-granular activated carbon
538 (MF-GAC)/nano filter hybrid system in high quality water reuse. Journal of
539 Membrane Science 476, 1-9.

540 Smith, A.L., Stadler, L.B., Love, N.G., Skerlos, S.J. and Raskin, L. (2012) Perspectives
541 on anaerobic membrane bioreactor treatment of domestic wastewater: A critical
542 review. Bioresource Technology 122, 149-159.

543 Tatsi, K. and Turner, A. (2014) Distributions and concentrations of thallium in
544 surface waters of a region impacted by historical metal mining (Cornwall, UK).
545 Science of the Total Environment 473, 139-146.

546 Vincent, T., Taulemesse, J.M., Dauvergne, A., Chanut, T., Testa, F. and Guibal, E.
547 (2014) Thallium(I) sorption using Prussian blue immobilized in alginate capsules.
548 Carbohydrate Polymers 99, 517-526.

549 Vipin, A.K., Fugetsu, B., Sakata, I., Isogai, A., Endo, M., Li, M.D. and Dresselhaus,
550 M.S. (2016) Cellulose nanofiber backboned Prussian blue nanoparticles as
551 powerful adsorbents for the selective elimination of radioactive cesium. Scientific
552 Reports 6.

553 Wu, S.M., Xu, Y., Li, X.L., Tong, R.F., Chen, L., Han, Y.D., Wu, J.B. and Zhang, X. (2018)
554 Controlled Synthesis of Porous Hierarchical ZnFe2O4 Micro-/Nanostructures with
555 Multifunctional Photocatalytic Performance. Inorganic Chemistry 57(24), 15481-
556 15488.

557 Xiao, K., Liang, S., Wang, X.M., Chen, C.S. and Huang, X. (2019) Current state and
558 challenges of full-scale membrane bioreactor applications: A critical review.
559 Bioresource Technology 271, 473-481.

560 Xu, H.Y., Luo, Y.L., Wang, P., Zhu, J., Yang, Z.H. and Liu, Z.M. (2019) Removal of
561 thallium in water/wastewater: A review. Water Research 165.

562 Yang, Y., Faustino, P.J., Progar, J.J., Brownell, C.R., Sadrieh, N., May, J.C., Leutzinger,
563 E., Place, D.A., Duffy, E.P., Yu, L.X., Khan, M.A. and Lyon, R.C. (2008) Quantitative
564 determination of thallium binding to ferric hexacyanoferrate: Prussian blue. Int J
565 Pharm 353(1-2), 187-194.

566 Yang, Y., Xiong, Z., Wang, Z., Liu, Y., He, Z.J., Cao, A.K., Zhou, L., Zhu, L.J. and Zhao,
567 S.F. (2021) Super-adsorptive and photo-regenerable carbon nanotube based
568 membrane for highly efficient water purification. Journal of Membrane Science

621.

Zhang, G.S., Fan, F., Li, X.P., Qi, J.Y. and Chen, Y.H. (2018a) Superior adsorption of thallium(I) on titanium peroxide: Performance and mechanism. Chemical Engineering Journal 331, 471-479.

Zhang, H.L., Qi, J.Y., Liu, F., Wang, Z.X., Ma, X.M. and He, D. (2022) One-pot synthesis of magnetic Prussian blue for the highly selective removal of thallium(I) from wastewater: Mechanism and implications. Journal of Hazardous Materials 423.

Zhang, L., Wu, H.B., Madhavi, S., Hng, H.H. and Lou, X.W. (2012) Formation of Fe2O3 Microboxes with Hierarchical Shell Structures from Metal-Organic Frameworks and Their Lithium Storage Properties. Journal of the American Chemical Society 134(42), 17388-17391.

Zhang, X., Fang, X.F., Li, J.S., Pan, S.L., Sun, X.Y., Shen, J.Y., Han, W.Q., Wang, L.J. and Zhao, S.F. (2018b) Developing new adsorptive membrane by modification of support layer with iron oxide microspheres for arsenic removal. Journal of Colloid and Interface Science 514, 760-768.

Zhao, Z., Xiong, Y.H., Cheng, X.K., Hou, X., Yang, Y.X., Tian, Y.P., You, J.L. and Xu, L. (2020) Adsorptive removal of trace thallium(I) from wastewater: A review and new perspectives. Journal of Hazardous Materials 393.

Zuo, K.C., Chen, M.S., Liu, F.B., Xiao, K., Zuo, J.L., Cao, X.X., Zhang, X.Y., Liang, P.

589 and Huang, X. (2018) Coupling microfiltration membrane with biocathode
590 microbial desalination cell enhances advanced purification and long-term stability
591 for treatment of domestic wastewater. Journal of Membrane Science 547, 34-42.
592